



OPEN

Human parietal epithelial cells as Trojan horses in albumin overload

Giovanna Priante^{1✉}, Monica Ceol¹, Lisa Ganesello¹, Claudia Maria Radu², Rachele Mantese¹, Lucia Federica Stefanelli¹, Martina Cacciapuoti¹, Francesca K. Martino¹, Lorenzo Arcangelo Calò¹, Franca Anglani¹, Federico Nalesso¹ & Dorella Del Prete¹

Parietal Epithelial Cells (PECs) activation and proliferation are common to several distinct forms of glomerulopathies. Due to several stimuli, PECs can change to a progenitor (CD24⁺ and CD133/2⁺) or a pro-sclerotic (CD44⁺) phenotype. In addition, PECs, which are constantly exposed to filtered albumin, are known to be involved in albumin internalization, but how this mechanism occurs is unknown. We hypothesized that PECs can transport albumin via receptor-mediated endocytosis and that albumin overload may affect the state of PECs. Conditionally immortalized human PECs (hPECs) were incubated with different albumin concentrations at different times. Albumin internalization studies were performed. Protein expression was assessed using In-Cell Western and immunofluorescence. Cell morphology was analyzed by phase-contrast microscopy and F-actin staining. We demonstrate that hPECs internalize albumin via receptor-mediated mechanisms. Under albumin stimulation, megalin, cubilin, CIC-5, CD133/2, CD24, and CD44 were upregulated. The increase of pERK1/2, the upregulation of ROCK1, ROCK2, caspase -3, -6, and -7, and the morphological changes associated with loss of F-actin fibers indicated that inflammation, proliferation and apoptosis mechanisms had been activated. Our results demonstrate that long-term exposure to high doses of albumin induces up-regulation of molecules involved in the tubular protein uptake machinery and suggest that albumin overload is able to trigger a regenerative process as well as an activation state which might lead in vivo to glomerular crescent formation.

Keywords hPECs, Albumin, CIC-5, Megalin, Cubilin, CD44

Human Parietal Epithelial Cells (hPECs) have received attention in recent years due to their localization and involvement in the pathogenesis of fibrotic lesions^{1,2}. They are located in the outer membrane of Bowman's capsule and may be characterized using specific markers. Mature PECs are recognizable by the expression of annexin A3 (ANXA3), LKIV69, Pax-2, Pax-8, and claudin³⁻⁵. PECs are very reactive in many glomerular diseases and even undergo robust proliferation in the glomerular basement membrane disease (anti-GBM disease), in diseases of endothelial cells (anti-neutrophil cytoplasmic antibody and pauci-immune glomerulonephritis), and in the focal segmental glomerulosclerosis (FSGS)⁶.

PECs and podocytes share a common embryological cell lineage, but, while podocytes (Podocalyxin⁺) are terminally differentiated, mature PECs (ANXA3⁺) are not, and retain low levels of proliferation under non-diseased conditions⁷. PECs characterization is evolving rapidly, stimulated by exciting new discoveries regarding their morphology, molecular phenotype, function, and cellular responses⁸. PECs can be considered as major players in glomerulonephritis. PECs are the main cell type populating glomerular crescents due to their activation process characterized by the CD44 positivity and by increased capacity for proliferation, migration, and extracellular matrix production⁹.

Given its localization, PECs are constantly subjected to low levels of filtered albumin which instead increase in nephrotic states. The ability of PECs to internalize albumin is well-known in animal models⁷, and the localization of human serum albumin in PECs has been reported also in human biopsies³. It is known that PECs perform albumin endocytosis⁶ but, to date, no data have been provided on how this mechanism occurs. Recently we have demonstrated in kidney biopsies of proteinuric patients with lupus nephritis (LN) the presence of PECs expressing CIC-5, megalin, and cubilin³. CIC-5, megalin and cubilin are part of the macromolecular complex involved at proximal tubular level in the endocytotic re-uptake of the low-molecular-weight proteins (LMWP) including albumin¹⁰. In biopsies of patients with LN we demonstrated the presence of two sub-population of hypertrophic PECs ANXA3⁺/Podocalyxin⁻/CD44⁻, both expressing CIC-5, megalin, and cubilin

¹Kidney Histomorphology and Molecular Biology Laboratory, Nephrology Unit, Department of Medicine - DIMED, University of Padua, Via Giustiniani 2, 35128 Padua, Italy. ²Thrombotic and Haemorrhagic Diseases Unit, Department of Medicine-DIMED, University of Padua, Padua, Italy. ✉email: giovanna.priante@unipd.it

and located at the tubular pole: one population was positive for progenitor marker CD 24 (CD24⁺), and negative for human serum albumin (HSA⁻) and for proximal tubular cell brush border marker Lotus Tetragonolobus Lectin (LTA⁻), thus resembling human adult parietal epithelial multipotent progenitors (APEMP)^{11,12}; the other was committed toward a proximal tubular phenotype being CD24⁻/HSA⁺/LTA⁺. These observations underline the great plasticity of these cells and suggest that they can change their morphology and protein expression in response to different stimuli (ischemia, proteinuria, hyperglycemia)⁴.

Our working hypothesis is that hPECs can transport albumin via receptor-mediated endocytosis and that albumin overload may affect the state of PECs. For this purpose, we choose to perform an in vitro study that mimicked what happens in patients with proteinuric glomerulonephritis, but without confounding elements such as pharmacological treatment that might influence the level of proteinuria.

We focused on the effect of albumin on hPECs to clarify whether components of the typical tubular protein uptake system, such as megalin, cubilin and CIC-5 are involved in the mechanism of albumin internalization. In addition, we have investigated how albumin overload can affect the expression of this system, and whether albumin overload, a condition that mimics the nephrotic state in humans, is able to induce phenotypic changes in hPECs.

Results

Human PECs internalize albumin in vitro

Human PECs (hPECs) were stimulated overnight with a low dose (10 µg/ml) of albumin-fluorescein isothiocyanate conjugate (FITC-BSA). hPECs confirmed the ability to internalize albumin (Fig. 1). Albumin internalization was detected as green endocytic vesicles located mainly in the perinuclear region.

Mechanism of albumin internalization

To assess which mechanism underlies the albumin uptake process, hPECs were incubated with increasing concentrations of FITC-BSA (10 µg/ml, 50 µg/ml, 100 µg/ml, 500 µg/ml and 1000 µg/ml) both at 37 °C (which promotes endocytosis) or at 4 °C (which inhibits endocytosis). These concentrations include the physiologic range⁷. Fluorescence intensity was recorded 30 min and 2 h after stimulation at both temperatures.

The analysis of FITC-BSA uptake assessed at 37 °C at both 30 min and 2 h showed a curve with a flattening characteristic of the plateau phase due to the saturation of the binding sites, a profile suggesting the presence of a receptor-associated uptake mechanism (Fig. 2A, continuous line). Uptake of BSA was significantly inhibited by treating hPECs with 100-fold excess of unlabeled BSA (uBSA) ($p < 0.05$ at 10 µg/ml, $p < 0.005$ at all the other concentrations) (Fig. 2A, dotted line). These results further indicated that FITC-BSA could be internalized via a receptor-mediated mechanism.

The results obtained from experiments performed on hPECs, at 4 °C are showed in Fig. 2B. At this low temperature, the intracellular fluorescence did not increase as a function of concentrations. Experiments at 4 °C confirmed that albumin adhered to the surface and that energy-dependent endocytotic processes did not take place at 4 °C.

Quantification of FITC-BSA uptake performed at 37 °C showed a significant dose-dependent increase at both 30 min and 2 h (Fig. 2C, $p < 0.0001$). Additionally, significant differences between 30 min and 2 h at 100 µg/ml ($p < 0.0001$), 500 µg/ml ($p < 0.005$), and 1 mg/ml ($p < 0.0001$) were observed (Fig. 2C). The amount of

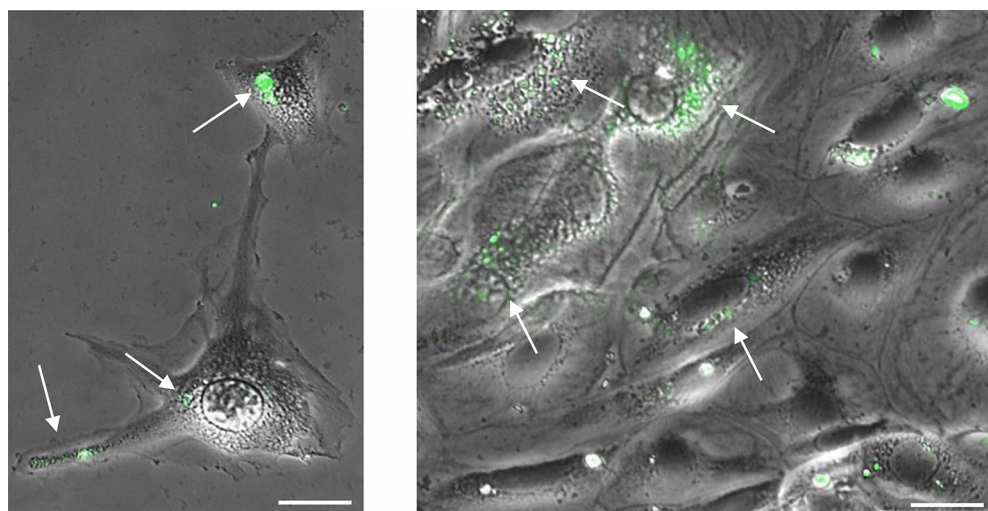


Fig. 1. Internalization of fluorescent albumin in hPECs. Images disclose the ability of hPECs to internalize albumin (FITC-BSA 10 µg/ml, 37 °C). Signals were detected as green vesicles (arrows). All images were acquired using a DMI6000CS-TCS SP8 fluorescence microscope (Leica Microsystems) placed within a temperature-controlled enclosure set at 37 °C and 5% CO₂ for live cell imaging. Images are representative of two separate experiments. Objective 20X/0.4. Scale bar 50 µm.

internalized albumin was higher at 37 °C compare to 4 °C and the difference was statistically significant at all concentrations (Fig. 2D).

These quantitative results were confirmed by visualization under a fluorescent microscopic (Fig. 2E,F). hPECs, incubated with 1 mg/ml of FITC-BSA for 2 h at 37 °C, were examined by confocal microscopy. FITC-BSA signal detected in hPECs (Fig. 2E) was significantly reduced after pre-treatment for 2 h with 100-fold excess of uBSA (Fig. 2F). Albumin vesicles were not seen at 4 °C (data not shown).

Human PECs express the macromolecular albumin uptake system

Since our results indicated that a receptor-mediated mechanism might be involved in albumin internalization, we looked in hPEC grown in standard conditions, for the presence of megalin, cubilin, and CIC-5, which are part of the macromolecular albumin uptake system normally present at tubular level. We demonstrated by immunofluorescence (IF), that the positivity for ANXA3 was present in all cells, confirming that they were mature hPECs (ANXA3⁺, Fig. 3A). In these hPECs we disclosed the presence of CIC-5, megalin and cubilin (Fig. 3B–D).

Confocal microscopic analysis was also performed (Fig. 3E–G) to better identify CIC-5, megalin and cubilin localization in hPECs. CIC-5 signal was detected at cytoplasmatic level (Fig. 3E). The labeling for megalin was located within hPECs at both cytoplasmatic and cell surface level (Fig. 3F). The same pattern was observed for cubilin (Fig. 3G). The labeling intensity of CIC-5, megalin and cubilin varied from area to area (Fig. 3F,G).

Colocalization of FITC-BSA, megalin, and cubilin in hPECs

The possible relationship between FITC-BSA uptake and megalin or cubilin expression was studied by double-labeling immunofluorescence on hPECs grown on chambers slide. hPECs were incubated with 1 mg/ml of FITC-BSA for 2 h at 37 °C, and then visualized by confocal microscopy. Colocalization of FITC-BSA with both megalin (Fig. 4A) and cubilin (Fig. 4B) was observed in hPECs (yellow/orange signal, Fig. 4, merge images).

BSA uptake inhibition

To verify the role of megalin and cubilin in albumin endocytosis, the uptake of FITC-BSA was investigated in the presence of a known inhibitor of megalin, such as a receptor-associated protein (RAP)^{13,14}, and using anti-human Cubilin IgG antibody to block the receptor binding^{14,15}. Differentiated hPECs were preincubated with different concentration (0.75, 1, 1.5, 2 and 3 µM) of Rap for 1 h or with different amounts (0.7, 1.5, 3, and 6 µg/ml) of a sheep polyclonal anti-human Cubilin IgG antibody for 3 h, followed by co-incubation with 1 mg/ml FITC-BSA for further 2 h.

As shown in Fig. 5A, RAP was able to inhibit uptake of FITC-BSA in a dose-dependent manner, achieving significance at 1.5 µM ($p < 0.0001$, 28% inhibition), 2 µM ($p < 0.0001$, 32.3% inhibition) and 3 µM ($p < 0.0001$, 37% inhibition).

Uptake was also inhibited in a dose-dependent manner by a sheep polyclonal anti-human Cubilin IgG antibody with significant inhibition at 1.5 µg/ml ($p < 0.0001$, 40% inhibition), 3 µg/ml ($p < 0.0001$, 43.2% inhibition) and 6 µg/ml ($p < 0.0001$, 51% inhibition) (Fig. 5B). These results agree with those obtained by immunofluorescence analysis. As showed in Fig. 5C, FITC-BSA alone showed diffused green signals within hPECs, which were greatly reduced by the addition of RAP (middle image) and specific antibody against cubilin.

Taken together, these results further strengthen the link in hPECs between albumin endocytosis and the macromolecular complex normally involved in the endocytotic uptake of albumin in human proximal tubular cells.

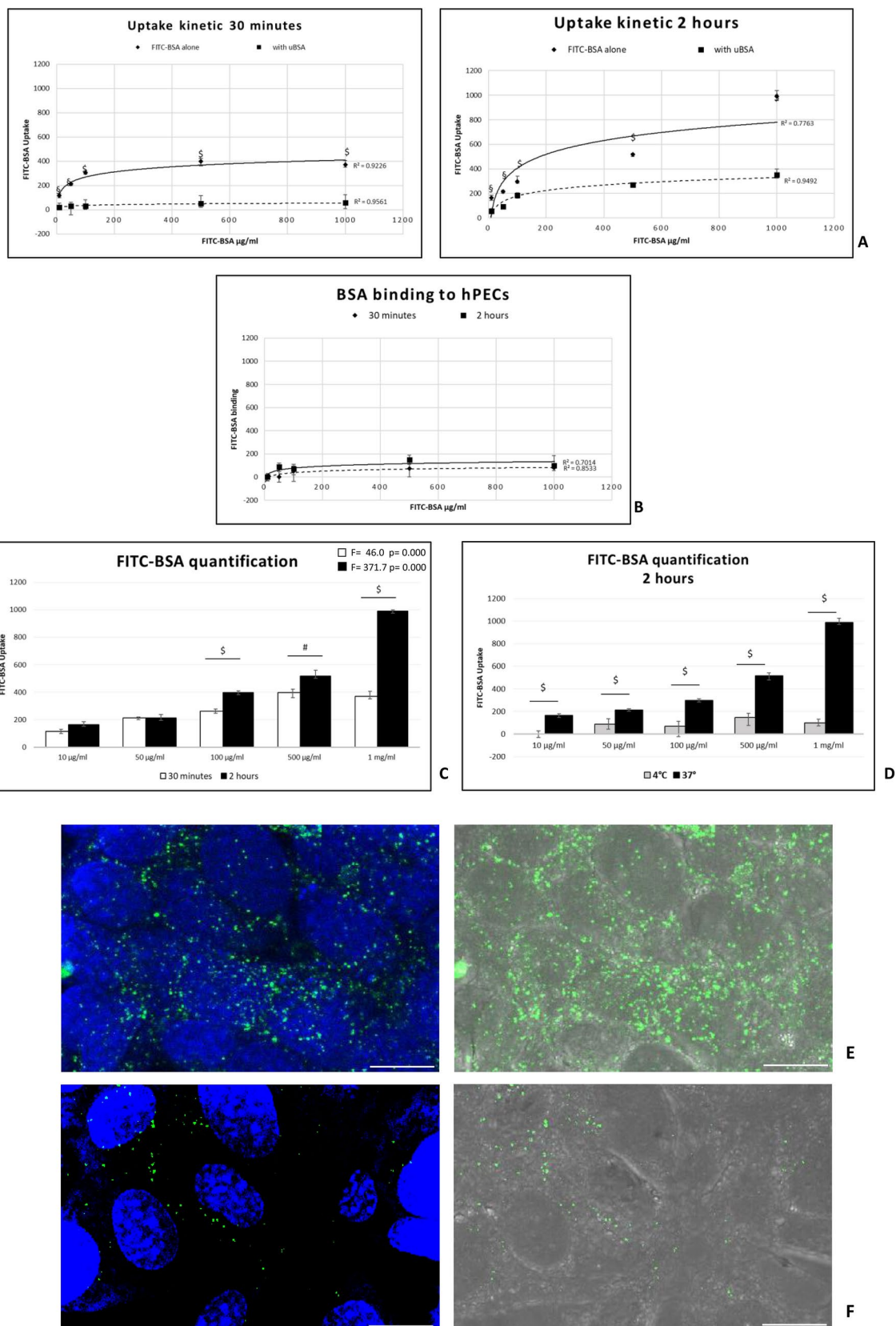
Albumin overload increases megalin, cubilin and CIC-5 protein expression

To determine whether the effect of protein overload on hPECs could induce a change on the megalin, cubilin, and CIC-5 protein expression, we performed In Cell Western (ICW) analysis (Supplementary Figure S1) on hPECS stimulated with 10 and 30 mg/ml of BSA for 48 and 72 hours.

Albumin treatment induced a significant increase in the expression of megalin at both 48 and 72 h with 10 mg/ml ($p < 0.05$ 48 h, $p < 0.01$, 72 h) and 30 mg/ml ($p < 0.01$ both) of albumin (Fig. 6). For megalin, clear dose-dependent stimulation was observed at 72 h (10 mg/ml vs 30 mg/ml, $p < 0.01$) (Fig. 6) and time-dependent stimulation at the 30 mg/ml concentration (48 vs 72 h, $p < 0.01$). (Supplementary Figure S2). Cubilin showed a significant increase at 48 h only at 30 mg/ml ($p < 0.05$) (Fig. 6), while at 72 h it showed a significant increase at both concentrations tested compared to control ($p < 0.05$) (Fig. 6). Moreover, cubilin expression showed a significant difference between 10 mg/ml and 30 mg/ml of BSA after 48 h ($p < 0.05$). Stimulation with albumin did not appear to affect CIC-5 expression at 48 h at both concentrations studied, while at 72 h a significant increase was observed at 30 mg/ml ($p < 0.05$) compared to control and 10 mg/ml ($p < 0.05$). (Fig. 6).

Albumin overload affects human PECs' phenotype

Using ICW, we investigated whether albumin stimulation induced a change in the phenotype of hPECs toward a progenitor (CD24⁺ and CD133/2⁺) or pro-fibrotic (CD44⁺) state. ANXA3 expression was also evaluated. As shown in Fig. 7A, both albumin concentrations caused a significant increase in CD24 expression at 48 and 72 h compared to control ($p < 0.01$). In addition, the expression of CD133/2 also increased significantly at 48 h with the two concentrations of albumin tested ($p < 0.05$), markedly at 72 h ($p < 0.01$) (Fig. 7A). The same trend was observed for CD44 expression at 48 h at the concentration of 10 and 30 mg/ml ($p < 0.01$). At 72 h, a significant increase was observed only at 30 mg/ml ($p < 0.01$) compared to control (Fig. 7A). The changes observed in these markers did not affect the expression of ANXA3, which remained stable over time at all concentrations tested (Fig. 7B).



◀ **Fig. 2.** Uptake of fluorescent albumin in hPECs. (A) Showed FITC-BSA internalisation after incubation of hPECs with different concentration of FITC-BSA, at 37 °C alone (continuous line) or in presence of 100-fold excess of unlabeled BSA (uBSA, dotted line) after 30 min and 2 h. Albumin uptake follows receptor-mediated profile. FITC-BSA was significantly reduced by treatment with 100-fold excess of uBSA (dotted line). Data are represented as fluorescence absorbance values normalized to cell number. Results are from three different experiments in triplicate. Statistical analysis was carried out using Mann–Whitney U-test, * $p < 0.05$, ** $p < 0.005$. (B) Showed results from BSA binding experiments. hPECs were incubated with different concentration of FITC-BSA at 4 °C for 30 min and 2 h. (C) Showed FITC-BSA quantification in hPECs at 37 °C after 30 min and 2 h. Albumin uptake increased significantly in a dose-dependent manner both at 30 min than 2 h. Data are represented as fluorescence absorbance values normalized to cell number. Results are from three different experiments in triplicate. Statistical analysis was carried out using ANOVA and Bonferroni's correction $F = 371.7$, at 2 h, $p < 0.0001$; $F = 46.0$ at 30 min, $p < 0.0001$. A significantly difference was found between 30 min and 2 h at 100 µg/ml, 500 µg/ml and 1 mg/ml of FITC-BSA * $p < 0.005$, $^{\$}p < 0.0001$ (Mann–Whitney U-test). (D) Showed FITC-BSA quantification in hPECs at 4 °C and 37 °C after 2 h of treatment with different concentration of FITC-BSA. Data are represented as fluorescence absorbance values normalized to cell number. Results are from three different experiments in triplicate. A significantly difference was found between FITC-BSA at 4 °C versus 37 °C, $^{\$}p < 0.0001$ at all concentrations (Mann–Whitney U-test). (E, F) showed representative confocal images of cultured hPECs in presence of FITC-BSA (1 mg/ml) alone (E) or after pre-treatment (2 h) with 100-fold excess of uBSA (F). FITC-BSA appears in green cytoplasmic vesicles. DNA stained with DRAQ5™ is shown in blue. The images on the left are merge of fluorescence signals (FITC-BSA and nuclei); the images on the right bright field (differential interference contrast, DIC) and fluorescent signal of FITC-BSA. Objective 63X/1.4, oil immersion. Scale bar 50 µm. Images are representative of two separate experiments.

retraction, drastic cell rounding with loss of the typical elongated shape, and cell connection disappearance. These changes occurred in a time-dependent manner, and the most drastic expression of morphological changes was observed at 72 h (Fig. 8A).

Untreated hPECs showed F-actin filaments normally distributed as bundles of stress fibers along the cell axis, arranged neatly and unbranched, as visualized by phalloidin staining (Fig. 8B). After BSA treatment, hPECs showed differences in F-actin patterning that consisted of an alteration of fiber distribution that appeared to be dose-dependent: the orderly arranged stress fibers of the actin cytoskeleton were disrupted, and a redistribution of F-actin fibers toward the periphery was observed at 10 mg/ml (Fig. 8B), until complete derangement/disruption of the fibers with 30 mg/ml of albumin for 72 h.

CTR and hPECs treated with lower albumin dose (10 mg/ml) showed a similar actin quantification. (Fig. 8C). At the highest dose of albumin (30 mg/ml) a significant decrease of F-actin signal was detected compared to CTR and to 10 mg/ml ($p < 0.005$) (Fig. 8C). No difference in cells number counted was evidenced between untreated and treated hPECs, confirming that the decrease in actin fluorescence was real and not linked to a reduction in cells population.

Albumin overload increases ROCK1/2 expression in hPECs

RhoA-ROCK signaling is known to control cellular behaviors such as morphology, proliferation, motility, adhesion and cell death^{16,17}. In our in vitro model, we analyzed the protein expression of ROCK1 and ROCK2 by ICW at 72 h. ROCK1 and ROCK2 exhibited similar patterns: their expression showed significant dose-dependent up-regulation (CTR vs 10 mg/ml, CTR vs 30 mg/ml, $p < 0.0001$ and 10 mg/ml vs 30 mg/ml $p < 0.0001$), with a more marked increase of ROCK1 than ROCK2 (Fig. 9).

Albumin overload upregulates effector caspases in hPECs

hPECs morphology changes in the presence of albumin overload led us to assess whether apoptosis was occurring. Since apoptosis is characterized by caspase activation, the levels of cleaved caspase-3, -6, -7 (effector caspases) were measured by ICW analysis (Fig. 10). Cultured hPECs were exposed to increasing concentrations of BSA (10 and 30 mg/ml) for 72 h. A significant increase in caspase-3, -6 and -7 ($p < 0.0001$) was observed at the highest dose of BSA (30 mg/ml) compared with CTR and 10 mg/ml.

Albumin effect on hPECs viability

To rule out whether albumin could have any effect on proliferation, the number of living cells was estimated by methylene blue assay. hPECs were incubated for 24, 48 and 72 h with different concentrations of albumin: 10 µg/ml, 100 µg/ml, 1 mg/ml, 10 mg/ml and 30 mg/ml.

We observed a decrease in cell number starting from 1 mg/ml of albumin, which was significant only at 48 h ($p < 0.005$ vs CTR) and 72 h ($p < 0.0001$ vs CTR). At 48 and 72 h, cell numbers at 10 mg/ml ($p < 0.0001$ for both time points) and 30 mg/ml ($p < 0.0001$ for both time points) were still significantly reduced. Moreover, at 30 mg/ml the decrease in cell number was significant at 72 h versus 48 h ($p < 0.0001$) (Supplementary Figure S3).

Albumin overload modulates pERK1/2 expression

It has been demonstrated that albumin internalization and subsequent apoptosis occurs in murine PECs after albumin overload exposure, and that p-ERK1 and 2 were involved⁷. Therefore, the levels of phosphorylated extracellular signal-regulated kinase 1 and 2 (p-ERK1/2) were examined in our in vitro model of hPECs following albumin overload treatment (10 and 30 mg/ml, 72 h). Phosphorylated ERK1/2 (pERK) were quantified using

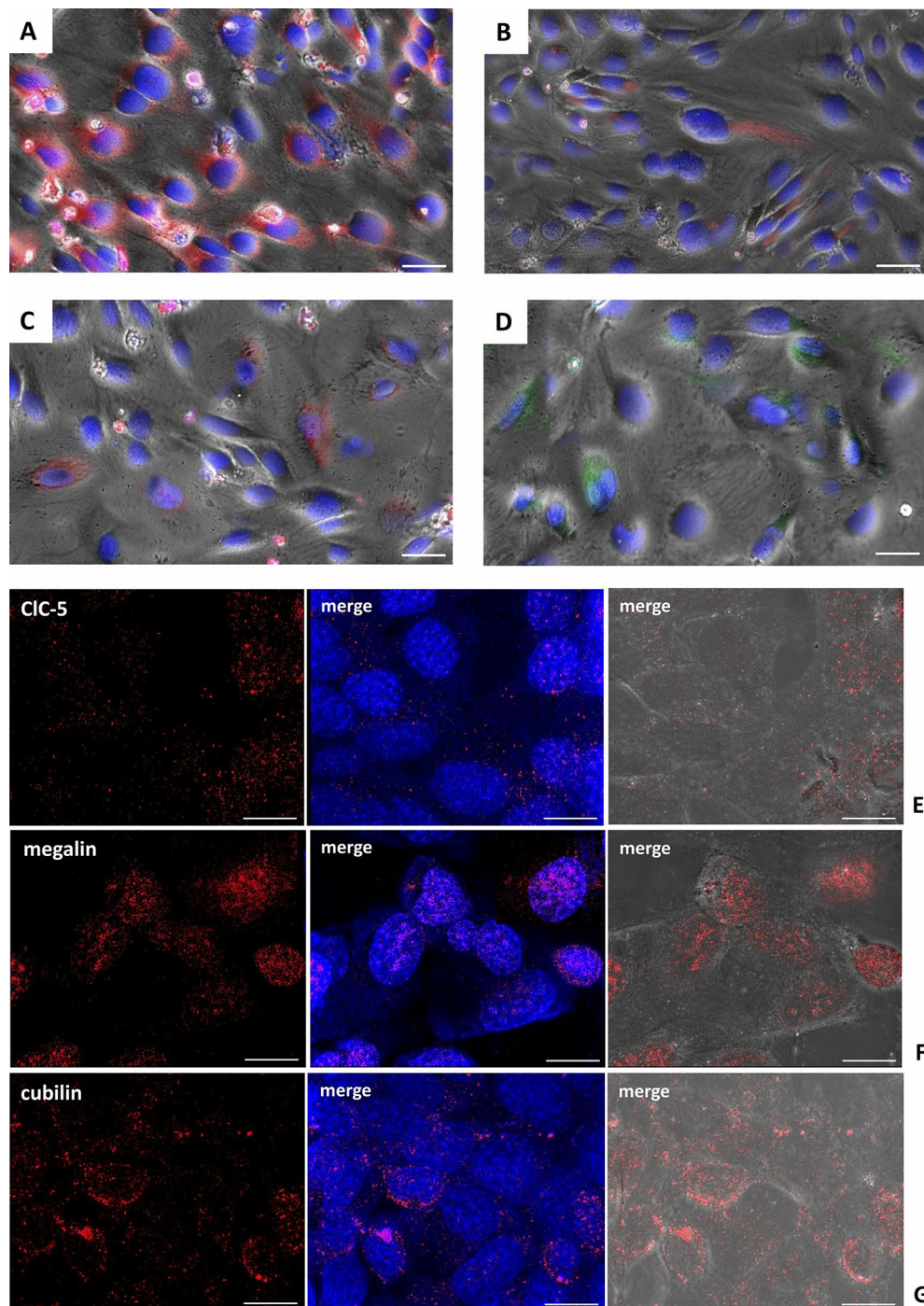


Fig. 3. hPEC express the macromolecular albumin uptake system. (A–D): Immunostaining of representative images of hPEC disclosing: (A) ANXA3 (red), (B) CLC-5 (red), (C) megalin (red), (D) cubilin (green). Nuclei were counterstained with DAPI (blue staining). The images are the overlay of the bright field and fluorescent signals. Positivity for ANXA3 was present in all cells, confirming that we had mature PECs. The positivity for CLC-5, megalin and cubilin was present in some but not all PECs. Images are representative of two separate experiments. Objective 20X/0.4. Scale bar 50 μ m. (E–G) representative confocal images of hPEC disclosing: (E) CLC-5, (F) megalin, (G) cubilin. All markers are shown in red (Alexa Fluor™ 594) (Left images); DNA stained with DRAQ5™ is shown in blue. The images on the middle are merge of fluorescence signals (markers and nuclei). The images on the right are the overlay of bright field (differential interference contrast, DIC) with fluorescent signal of the different markers. Images are representative of two separate experiments and were analysed by a fluorescence microscope DMI6000CS-TCS SP8 (Leica Microsystems) in confocal mode, with a Z-interval of 1 μ m z-interval. Objective: 63X/1.4, oil immersion. Scale bar = 50 μ m.

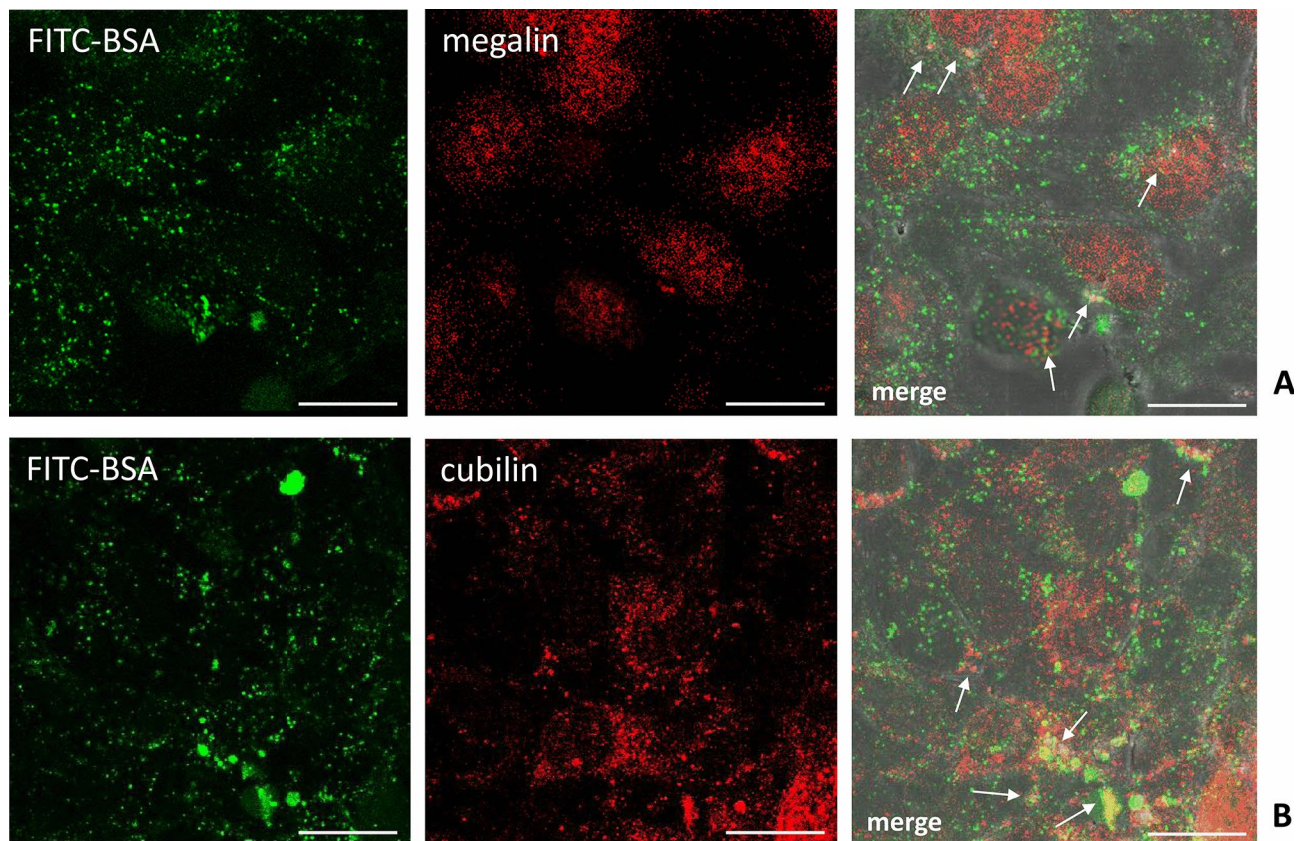


Fig. 4. Immunofluorescence microscopy of colocalization of FITC- BSA and megalin or cubilin. Representative immunofluorescent images by confocal microscopy showed protein expression and colocalisation of megalin (**A**) and cubilin (**B**) with FITC-BSA. FITC-BSA is shown in green, megalin (**A**, Alexa Fluor™ 594) and cubilin (**B**, Alexa Fluor™ 594) in red. In merge images white arrows indicate colocalization as yellow/orange signal. Images are representative of two separate experiments and were analysed by a fluorescence microscope DMI6000CS-TCS SP8 (Leica Microsystem) in confocal mode, with a Z-interval of 1 μ m z-interval. Objective: 63X/1.4, oil immersion. Scale bar = 50 μ m.

ICW. Phosphorylated ERK1 and 2 were significantly increased only at 30 mg/ml of albumin concentration compared to CTR ($p < 0.005$) (Fig. 11).

Discussion

Parietal epithelial cells are a heterogeneous cell population located on Bowman's capsule, forming a cell monolayer facing the urinary space with tight junctions between adjacent cells. These cells are known to internalize albumin^{6,7}, but the mechanism underlying this activity has not yet been elucidated. The aim of our study was first to understand whether components of the protein uptake machinery (CIC-5, megalin and cubilin), normally expressed at tubular level, could play a role in hPECs, and, second, to evaluate how hPECs respond to albumin overload.

With this in vitro study, we demonstrate that hPECs are able to internalize albumin, forming vesicles through a process of endocytosis. Our results are consistent with what has already been observed in mouse and rat PECs in vitro and in vivo⁷ and in human biopsies³. To establish the mechanism of albumin uptake in hPECs, endocytosis and binding assays were performed. Experiments performed in excess of unlabelled BSA showed that uptake was inhibited, demonstrating specificity of the binding. The observation that albumin internalization was higher at 37 °C strongly points to an active, energy-dependent process of albumin uptake. All together these results demonstrated a receptor-mediated endocytosis.

Recently, we have revealed the presence of CIC-5, megalin and cubilin in PECs of patients with lupus nephritis³. In this in vitro study we have investigated the possibility that megalin and cubilin receptors could be involved in albumin uptake. Experiments of colocalization and inhibition of megalin and cubilin have strengthened this hypothesis, providing clear evidence for the involvement of these receptors in albumin endocytosis by hPECs. Albumin uptake was most inhibited by the blockade of the cubilin receptor, suggesting that cubilin, as documented in podocyte¹⁵ and proximal tubule cells¹⁸, might be the major player in the process of albumin endocytosis in hPECs as well. Moreover, up-regulation of megalin, and cubilin protein expression was observed in overload conditions. CIC-5 was upregulated at the longest time and highest dose considered, suggesting that protein overload in hPECs first affects the expression of megalin and cubilin, then involves the

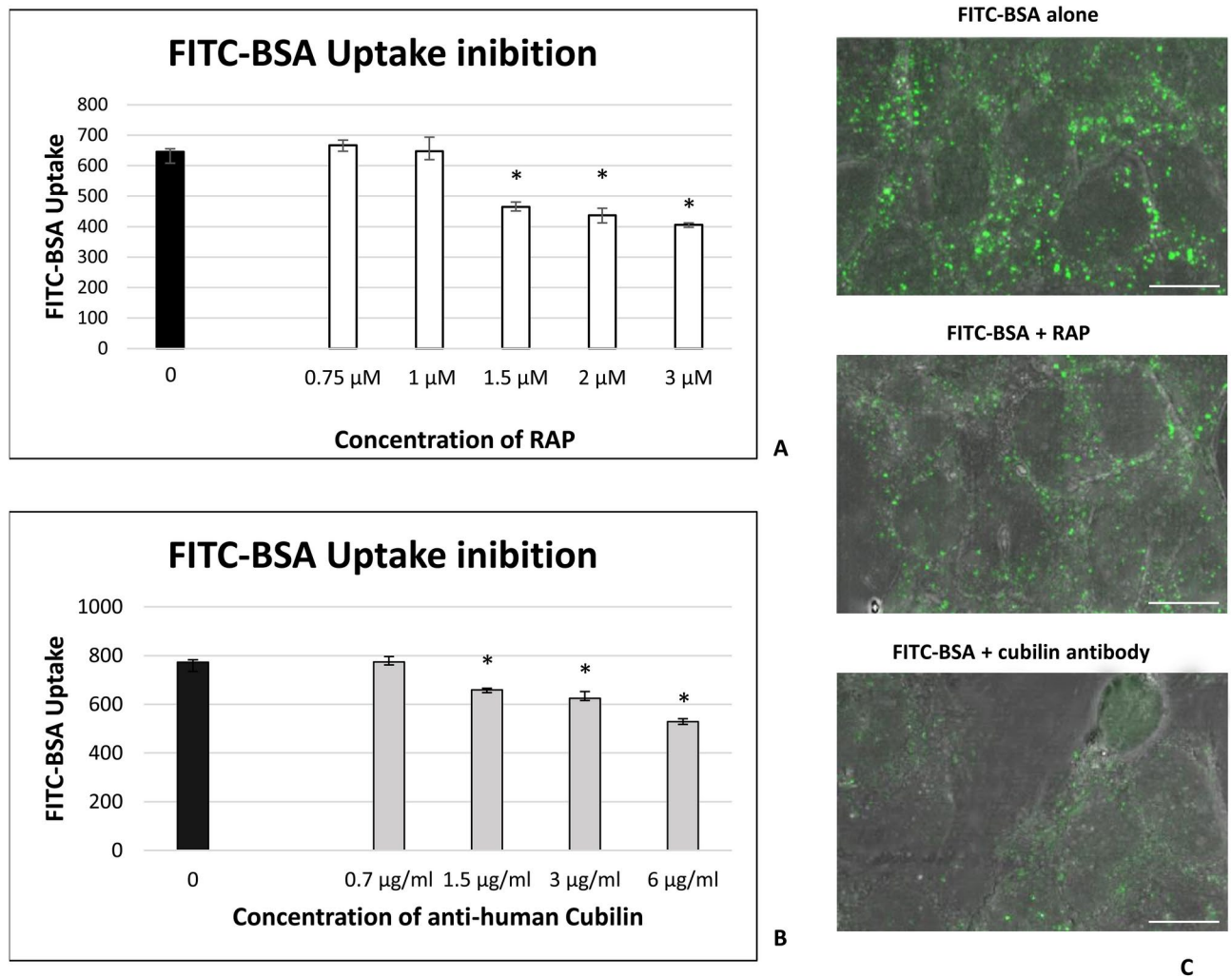


Fig. 5. Inhibition of BSA-FITC uptake. (A) Effect of receptor-associated protein (RAP) on FITC-BSA uptake in hPECs. hPECs were preincubated with different amounts of RAP for 1 h (white bargraphs) followed by incubation with 1 mg/ml FITC-BSA for 2 h. Black bargraphs display FITC-BSA alone. Data are represented as fluorescence absorbance values normalized to cell number. Results are from two independent experiments performed in triplicate * $p < 0.05$ (Mann–Whitney U-test). (B) Effect of a sheep polyclonal anti-human Cubilin IgG antibody on FITC-BSA uptake in hPECs. hPECs were preincubated with different amounts of a sheep polyclonal anti-human Cubilin IgG antibody for 3 h (gray bargraphs) followed by incubation with 1 mg/ml FITC-BSA for 2 h. Black bargraphs display FITC-BSA alone. Data are represented as fluorescence absorbance values normalized to cell number. Results are from two independent experiments performed in triplicate * $p < 0.05$ (Mann–Whitney U-test). (C) Representative confocal images of inhibition by RAP and a sheep polyclonal anti-human Cubilin IgG antibody on FITC-BSA uptake. FITC-BSA was detected as green signal. Images are representative of two separate experiments and were analysed by a fluorescence microscope DMI6000CS-TCS SP8 (Leica Microsystem) in confocal mode, with a Z-interval of 1 μ m z-interval. Objective: 63X/1.4, oil immersion. Scale bar = 50 μ m.

ClC-5 chloride channel Cl⁻/H⁺ exchanger in the endocytic vesicle acidification. This pattern of expression in hPECs further support the link between the albumin uptake and the macromolecular system. Our data confirm previous results obtained in human podocytes¹⁵. The signaling and trafficking of cellular receptors are highly interlinked processes. We recognize that our study lacks information on other molecules normally involved in the macromolecular uptake system of the proximal tubule, such as Dab2, AMN.

Our hypothesis is that hPECs could act as a “second barrier” in the proteinuric *milieu* to counteract protein overload. We argue that the purpose of this mechanism could be to prevent albumin from spilling into the extraglomerular space where it would induce periglomerular inflammation.

PECs have been thoroughly studied for their regenerative potential. Romagnani’s group identified PECs in human kidneys expressing podocyte markers, known as ‘parietal podocytes’, adjacent to the vascular pole^{11,19}. Adult parietal epithelial multipotent progenitors close to the tubular pole expressing CD24 and CD133/2, but neither podocytes nor tubular markers have also been identified¹⁹. Our results demonstrate that albumin overload induces hPEC to up-regulate CD133/2 and CD24 stem cell markers, thus inducing a change in their

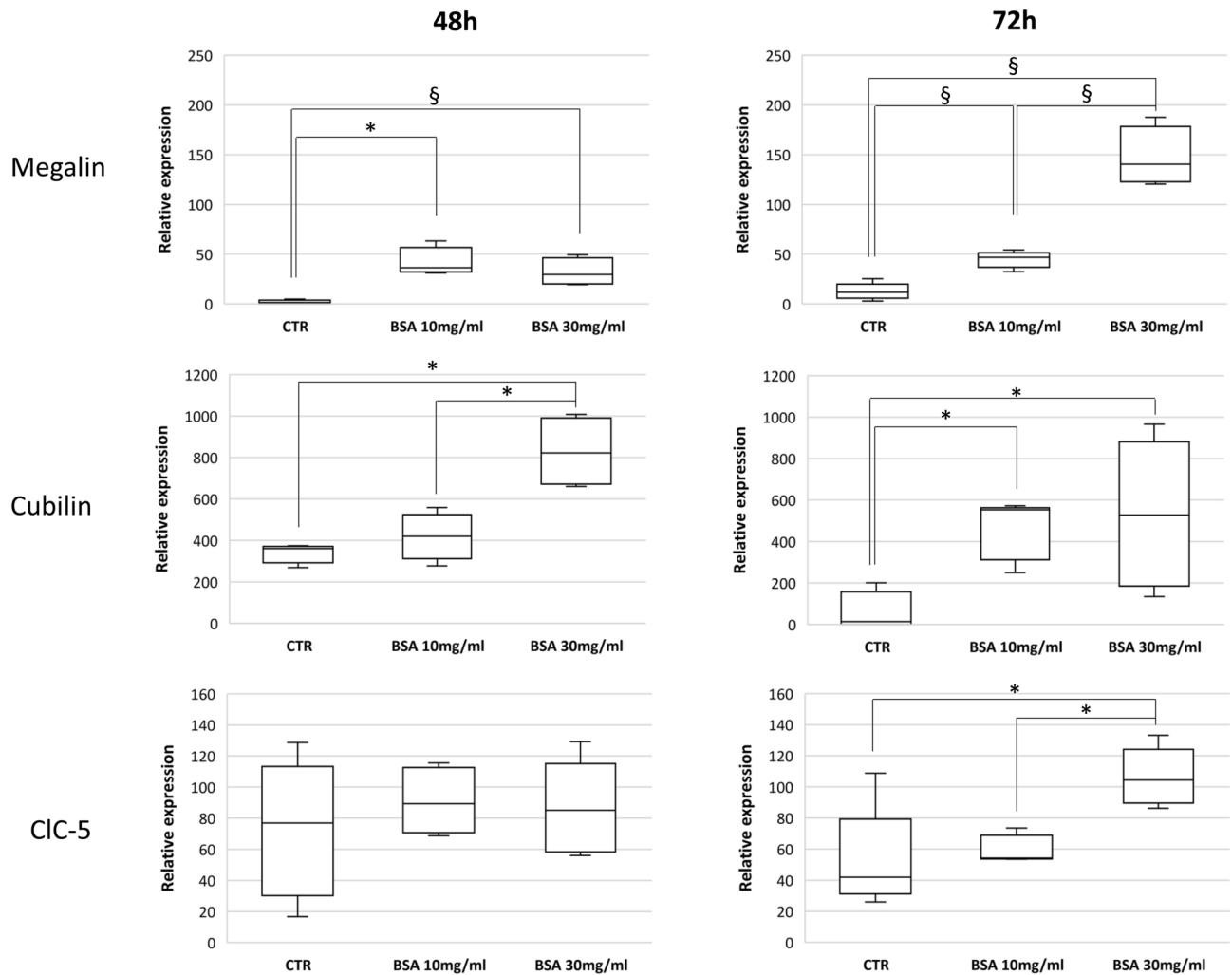


Fig. 6. Protein expression of the macromolecular albumin uptake system under albumin overload. Protein expression analysis was performed by ICW. Data are represented as absorbance values normalised to cell number. Results are from two independent experiments performed in triplicate. CTR: unstimulated control cells, * $p < 0.05$, § $p < 0.01$ (Mann–Whitney U-test).

phenotype, and to increase CD44 positivity, therefore supporting evidence of a heterogeneous population as previously reported in human biopsies³. These data suggest that proteinuric environment may induce hPECs to change their phenotype into two different lineages: a more immature one, resulting in increased capacity of self-regeneration, and a second one directed towards fibrosis and apoptosis. The absence of a change in ANXA3 expression levels suggests that the experimental timings used mimic the early stages of proteinuric nephropathy, thus resulting in the presence of an intermediate phenotype between mature and immature hPECs.

Several studies in animal and human kidneys have shown that CD44 is a specific marker of PECs activated towards a pro-sclerotic phenotype. These PECs can invade the capillary floccules and give rise to glomerulopathies characterized by fibrosis^{20,21}. In diabetic rats, it has also been showed that CD44 expression is induced by the internalization of high doses of albumin¹. Our in vitro model showed that even in hPECs, albumin overload leads to increased CD44 expression. However, we were unable to demonstrate cell proliferation in our model, although the increased ERK1/2 phosphorylation supports the activation of a profibrotic mechanism.

The presence of alterations in hPECs' morphology, cytoskeleton, and the change in phenotype markers induced by albumin, led us to explore whether there were modifications in growth behavior. In our study, hPECs showed a morphological change with an increasingly retracted and circular shape, and cell boundaries resembling those of loosely adherent cells with a rounded aspect depending on time and albumin concentration. These morphological aspects were associated with a redistribution of F-actin fibers, leading to non-adhesive membrane swelling, resulting in dysregulation of cell adhesion and flanking capacity, and cell membrane detachment and ultimately apoptosis. Increased p-ERK1/2 has also been shown to increase albumin-induced apoptosis in renal cells^{22–24}. The results obtained from our study on the expression of phosphorylated ERK1/2 in hPECs, suggest that this pathogenetic mechanism might contribute to shifting hPECs toward pro-fibrotic and pro-apoptotic phenotype upon prolonged albumin stress.

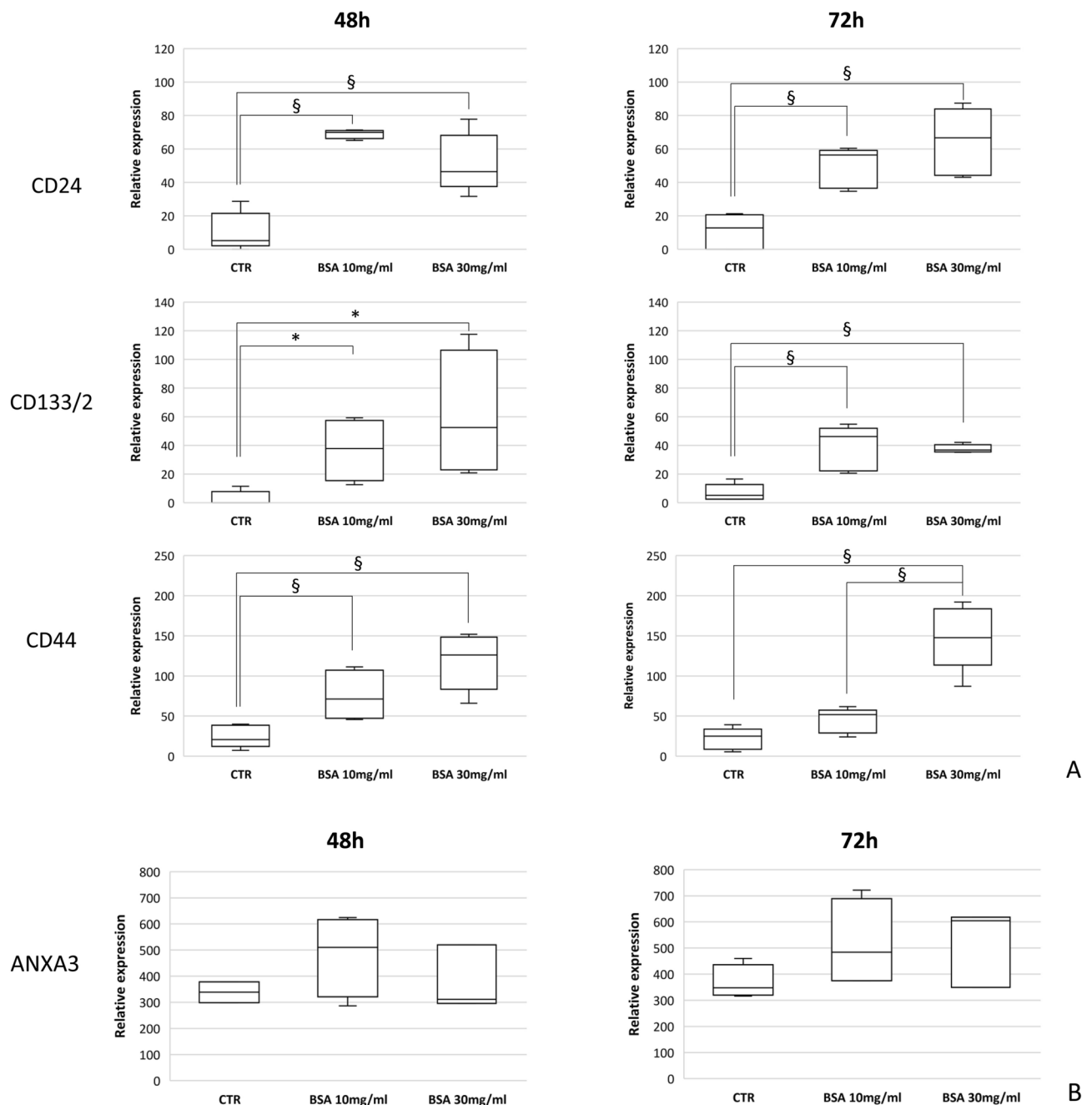


Fig. 7. Protein expression of hPECs markers. Protein expression analysis was performed by ICW. **(A)** Protein expression of CD24, CD133/2 and CD44 markers. **(B)** Protein expression of ANXA3 marker. Data are represented as absorbance values normalized to cell number. Results are from two independent experiments performed in triplicate. CTR: unstimulated control cells, * $p < 0.05$, § $p < 0.01$ (Mann–Whitney U-test).

The ROCK signaling pathway is involved in a variety of key biological processes and in managing cellular behavior^{16,17}. Important functions of the RhoA-ROCK pathway include: regulation of various transcription factors²⁵, remodeling of actomyosin cytoskeletal, control of stress fiber formation²⁶, stabilization of F-actin and network assembly²⁷, and stabilization of microtubule²⁸. ROCK 1 and ROCK 2 are cleaved by caspases during the induction of apoptosis process and are activated concomitantly^{29–31}. In our study the active ROCKs and executioner caspases (caspase-3, -6, and -7) were significantly up-regulated and accompanied by a reduction in cell number in a time and albumin dose-dependent manner. These results suggest that the initiation of the apoptotic process, resulting in changes in the shape of the cells and fiber alteration, is in response to the up-regulation of ROCK via caspase-3-dependent cleavage and activation of ERK-signaling^{29–33}.

Based on these data, we believe that hPECs could act as “frontline soldiers” to limit the injuries due to proteinuric milieu, by helping to remove albumin, and acting as a barrier. On the other hand, prolonged

exposure to albumin overload induces changes in the behavior of hPEC, inducing pathological pathways that lead to glomerular pathology. Considering the potential role of PECs in spreading injury within the glomerular capsule to subsequent segments, they might be more appropriately characterized as “Trojan horses” rather than “frontline soldiers”.

Our data are in agreement with *in vivo* studies suggesting that the transition from cellular crescents to fibrous crescents is linked with PEC altered behaviors such as those leading to fibrosis, apoptosis, and crescent formation that could be likely due to an oversupply epithelial repair response, driven by surviving PECs^{6,34,35}.

The results obtained in this *in vitro* study confirm those obtained in patients with LN where PECs expressing CLC-5, megalin, and cubilin were scattered around the glomerulus³. With our *in vitro* experiments, we observed the same distribution of megalin, cubilin and CLC-5 in a population of over 97% ANXA 3-positive PECs, as shown in Fig. 3, and for the first time we demonstrated an active role of megalin and cubilin in the mechanism of albumin uptake. Our study confirms that hPECs can express CD44, CD133 and CD24 in albumin overload condition as already shown in glomeruli of proteinuric patients. Proteinuric patients at the time of biopsy are usually under pharmacological treatment with drugs such as ACEi or angiotensin II type 1 receptor blockers that could affect proteinuria level, which led us to study parietal cells *in vitro* to understand their contribution in the mechanisms of albumin uptake without further interference. Our *in vitro* data highlight the active role of PECs in the protein uptake process.

In conclusion, our *in vitro* model showed that hPECs are able to internalize albumin through a receptor-mediated mechanism involving the well-known megalin and cubilin albumin receptors as well as CLC-5. To our knowledge, there are no data on the expression profile of this macromolecular system in hPECs under protein overload. Albumin overload acts on hPECs phenotype by inducing the expression of both stemness markers and activation toward a profibrotic phenotype. We have hypothesized that the dangerous insult triggered in hPECs a regenerative process and an activation state closely related to proliferation and migration, likely leading, *in vivo*, to crescent formation.

Materials and methods

Cells cultures

Human parietal epithelial cells (hPECs)

Human immortalized PECs (hPECs) were kindly provided by Professor Catherine Meyer-Schwesinger⁴. Cells were grown under permissive conditions (33 °C and 5% CO₂) in 1:1 mixture of endothelial growth medium (EGM) and RPMI 160. EGM was supplemented with 5% fetal bovine serum (FBS), 0.4% bovine brain extract, 0.1% hEGF, 0.1% hydrocortisone, 0.1% gentamicin and amphotericin B, 100 units/ml penicillin, 100 mg/ml streptomycin (Lonza, Basel, Switzerland), and RPMI 1640 (Sigma-Aldrich, St. Louis, MO, USA) with 10% FBS (F7524-Sigma-Aldrich), 1X ITS (Sigma-Aldrich), 2 mM L-glutamine and antibiotic mixture (Sigma-Aldrich). For differentiation, hPECs were cultured for 14 days under non-permissive conditions (37 °C and 5% CO₂) in 1:1 EGM and RPMI 1640 with supplements mentioned above. Cell density was kept at 90% to allow cell contact formation. hPECs were differentiated on collagen (Collagen I, Bovine, A10644-01, Gibco- ThermoFisher Scientific, Waltham, MA USA) coated plasticware. The end of the differentiation process was assessed on the grounds of hPEC's marker annexin A3 (ANXA3) positivity. Cells were used between passages 7 and 12.

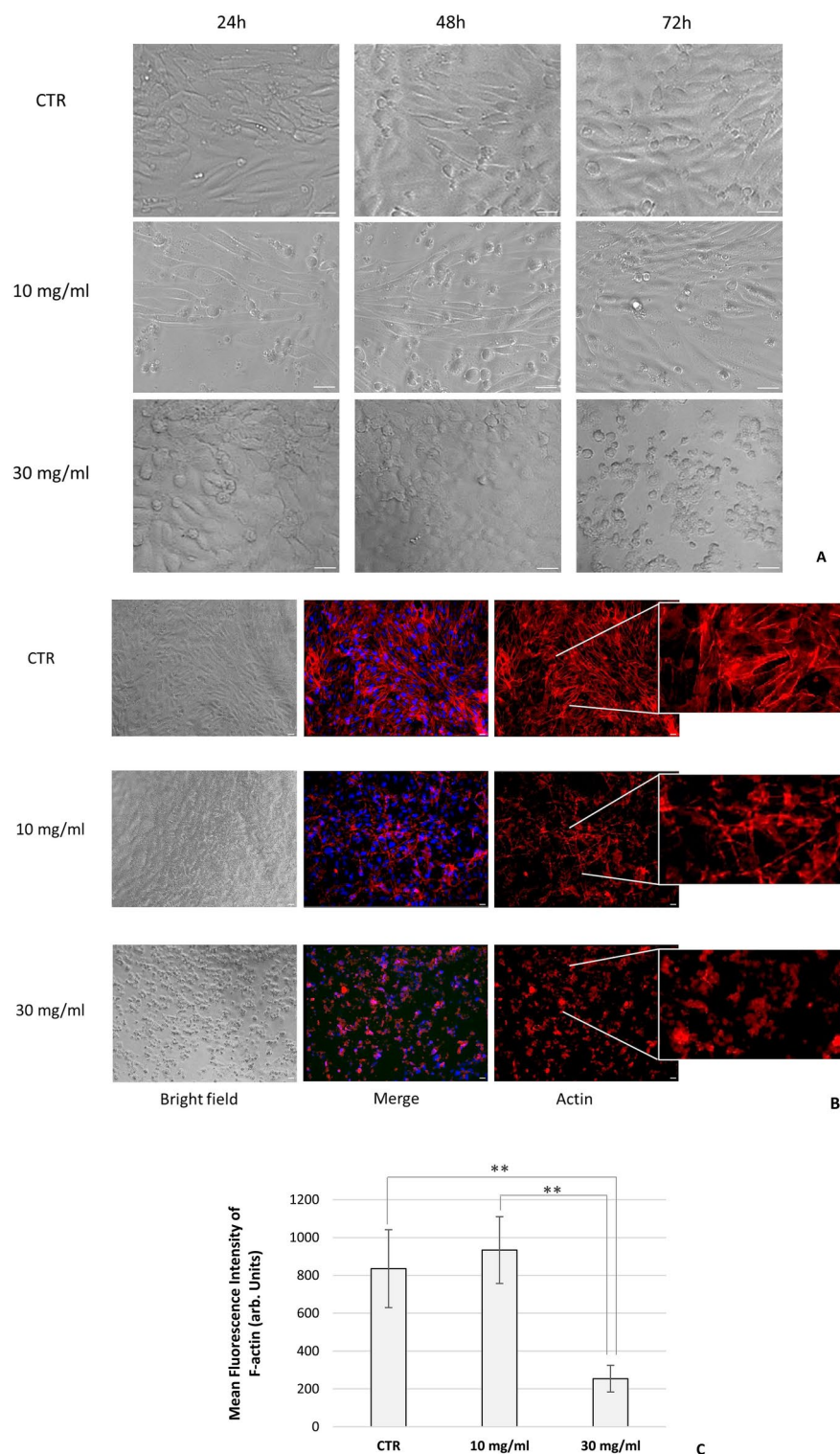
Immunofluorescence and confocal analysis

Immunofluorescence (IF) analyses was performed on hPECs as previously reported¹⁵. Mature hPECs were seeded on 8-well chamber slides and cultivated in standard conditions or with appropriate treatments. Cells were fixed with 2% paraformaldehyde in a 1X PBS buffer for 20 min at room temperature (RT). Cell membrane permeabilization was performed by incubating hPECs with a solution of Triton X-100 diluted 0.4% in 1X PBS, for 15 min at RT. Non-specific sites were blocked by incubating with 10% NDS (normal donkey serum, Abcam, Cambridge, UK) in 1X PBS for 30 min at RT. Samples were then incubated overnight with the appropriate primary antibody (Supplementary Table S1) diluted in 1X PBS 5% BSA at 4 °C. Samples were then incubated with the appropriate fluorescent secondary antibody (Supplementary Table S1) diluted in 1X PBS 5% BSA at RT. Nuclei were counterstained with 4',6-diamidino-2-phenylindole (DAPI, Vector Laboratories Burlingame, CA) diluted 1:1000 in 1X PBS for 5 min at RT. Negative controls were run by omitting primary antibody. Images were acquired with a DMI6000CS-TCS SP8 fluorescence microscope (Leica Microsystems, Wetzlar, Germany) with a 20X/0.4 objective using a DFC365FX camera (Leica Microsystems) and subsequently analyzed with the LAS-AF software v.3.1.1 (Leica Microsystems).

Confocal microscopy analysis was also performed. Samples were incubated overnight with the specific primary antibody (Supplementary Table S1) diluted in 1X PBS 5% BSA at 4 °C, and then incubated with the appropriate fluorescent secondary antibody: Alexa Fluor 597-conjugated donkey anti-rabbit megalin antibody (Life Technologies, Carlsbad, CA, USA), and Alexa Fluor 597-conjugated donkey anti-sheep Cubilin antibody (Life Technologies, Carlsbad, CA, USA) (Supplementary Table S1). Nuclei were counterstained with fluorescent DNA dye DRAQ5 (ab108410, Abcam, Cambridge, CB2 0AX, UK) diluted 1:500 in 1X PBS for 20 min at 37 °C. Negative controls were run by omitting primary antibody. Images were acquired with a DMI6000CS-TCS SP8 fluorescence-confocal microscope (Leica Microsystems, Wetzlar, Germany) with a 63X/1.4 objective using a DFC365FX camera (Leica Microsystems) and subsequently analyzed with the LAS-AF software v.3.1.1 (Leica Microsystems).

Albumin uptake and binding analysis

To verify albumin endocytosis *in vitro*, hPECs were seeded on 24-well plates and then incubated overnight with albumin-fluorescein isothiocyanate conjugate from bovine (FITC-BSA, A9771, Sigma Aldrich) 10 µg/ml in medium without phenol red. Images were acquired using an inverted fluorescence microscope Leica DMI600CS-



TCS SP8 (Leica Microsystems) equipped with an incubator, with a temperature-controller set at 37 °C and in a humified 5% CO₂ atmosphere, for live cell imaging. Images were analysed by Leica Application Suite (LAS-AF) v.3.1.1 software (Leica Microsystems). Experiments were run twice and acquired with 20X/0.4 objective using a DFC365FX camera (Leica Microsystems).

Cellular albumin uptake was quantified as described by Coffey et al.³⁶ with some modifications. Briefly, mature hPCECs seeded on 24-well plates were growth with medium 1:1 mixture of EGM and RPMI 1640 with supplements mentioned above but containing only 1% FBS for 24 h, to synchronize hPCECs in the same cell-cycle phase. After synchronization, differentiated hPCECs were incubated with increasing concentrations of FITC-BSA (10, 50, 100, 500 and 1000 µg/ml) for 30 min and 2 h at 37 °C alone or in presence of 100-fold excess of unlabeled BSA (uBSA). Intracellular fluorescence was measured in a single-beam fluorimeter (Victor X3, PerkinElmer, Boston Industries, Walpole, MA) at an excitation wavelength of 490±10 nm and emission wavelength of

Fig. 8. Evaluation of hPECs morphology after albumin overload. (A) Representative microscopy images of hPECs by differential interference contrast (DIC) (grey-scale images) showing cell shape changes at different time and albumin concentration. CTR: untreated cells. Images were acquired using a DMI6000CS-TCS SP8 fluorescence microscope (Leica Microsystems) with 40X/0.60 objective. Scale bar 50 μ m. (B) Phalloidin fluorescence labelling of F-actin in hPECs after albumin overload for 72 h. Images demonstrating the pattern of F-actin filaments distributed as bundles of stress fibers along the cell axis, arranged neatly and unbranched in untreated cells (CTR). Boxed photos showing zoomed-in area. Stress fibers of the actin cytoskeleton were disrupted: a marked redistribution of F-actin fibers toward the periphery was observed (10 mg/ml), markedly and completely unwrapped at the higher concentration (30 mg/ml). Red: actin; Blue: DAPI. Fluorescence microscope images are representative of three separate experiments. Images were acquired using a DMI6000CS-TCS SP8 fluorescence microscope (Leica Microsystems) with 20X/0.4 objective. Scale bar 50 μ m. Merge: phalloidin/actin with DAPI. Scale bar 50 μ m. (C) Quantification of F-actin intensity: data are reported as mean \pm SD of the measured gray-scale values of images from each condition and normalized to cell number counted on the same measured cell area. Results are from three independent experiments $**p < 0.005$, $F = 20.75$, using ANOVA and by Bonferroni's correction.

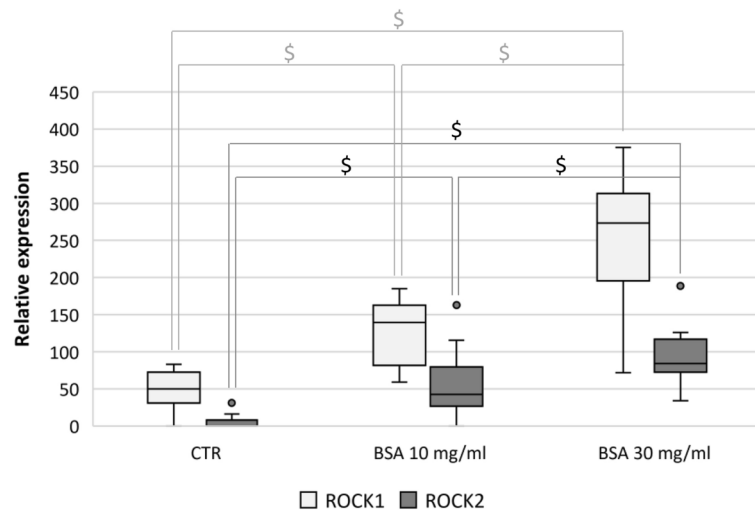


Fig. 9. Protein expression of ROCK1 and ROCK2 after albumin overload for 72 h. Protein expression analysis was performed by ICW. Data are represented as absorbance values normalized to cell number. Results are from two independent experiments performed in triplicate. CTR: unstimulated control cells, $^{\$}p < 0.0001$ (Mann–Whitney -test).

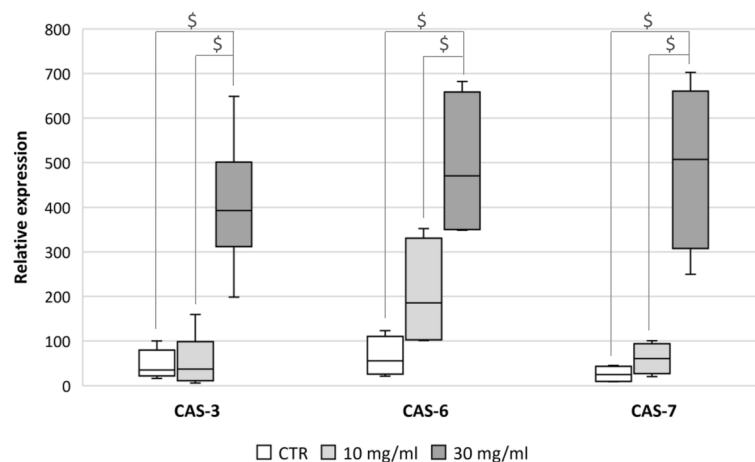


Fig. 10. Protein expression of cleaved Caspase -3, -6 and -7 after albumin overload for 72 h. Protein expression analysis was performed by ICW. Data are represented as absorbance values normalized to cell number. Results are from two independent experiments performed in triplicate. CTR: unstimulated control cells, $^{\$}p < 0.0001$ (Mann–Whitney -test).

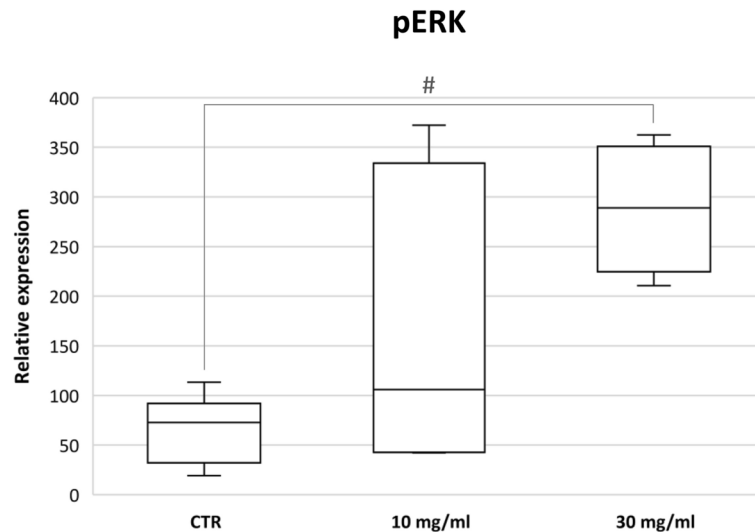


Fig. 11. Evaluation of pERK1/2 in hPECs under albumin overload for 72 h. The boxplots express the phosphorylated ERK1/2 evaluated by ICW. Data are represented as absorbance values normalized to cell number. Results are from two independent experiments performed in triplicate. CTR: unstimulated control cells, $^{\#}p < 0.005$ (Mann–Whitney U-test).

520 ± 10 nm. Fluorescence was normalized for the number of cells using 1% Methylene Blue assay³⁷. Cells were stained for 30 min with 1% methylene blue in 0.01 M borate buffer, pH 8.5. After repeated washing with borate buffer, the fixed stain was eluted with 0.1 N HCl/ethanol 1:1 (vol/vol). Absorbance (OD) was measured at 650 nm with the EnSight Multimode Plate Reader (Perkin Elmer). Methylene blue only stains cells attached to the substrate before fixation (i.e., living cells)^{37–39}. Results were expressed as ratio fluorescence/OD.

Binding of FITC-BSA was determined using the same procedure as for endocytotic uptake at 4 °C.

Effect of inhibitor on albumin endocytosis

Some experiments with potential competitors of uptake were performed. Human receptor-associated protein (hRAP) (Innovative Research, Novi, MI) and a sheep polyclonal antibody against cubilin (Supplementary Table S1)¹⁵ were used to inhibit albumin endocytosis. After 24 h in serum free medium, hPECs were preincubated for 1 h with different concentration (0.75 – 1 – 1.5 – 2 and 3 μM) of hRAP, or for 3 h with different concentration (0.7–1.5–3–6 μg/ml) of purified polyclonal anti-cubilin and then subsequently co-incubated with FITC-BSA 1 mg/ml for 2 h.

To assure that incubation at 37 °C promotes endocytotic uptake, experiments were also performed with hPECs differentiated on collagen type I-coated chamber slides and treated with FITC-BSA 1 mg/ml for 2 h. Cells were fixed by 2% paraformaldehyde in a 1X PBS buffer for 20 min, and the rinsed for 15 min with 1X PBS twice. The slides were viewed on the DMI6000CS-TCS SP8 fluorescence microscope (Leica Microsystems, Wetzlar, Germany) with a 20X/0.4 objective or 63X/1.4 oil immersion objective, using a DFC365FX camera (Leica Microsystems) and images were acquired.

BSA overload in vitro study

To evaluate albumin effects, we used an in vitro model of overload proteinuria. Differentiated cells were synchronized in the same cell-cycle phase by starvation in 1:1 EGM and RPMI 1640 medium, containing 1% FCS for 24 h. After synchronization, hPECs were incubated with BSA (A8412, Sigma) at 10 and 30 mg/ml concentrations for 48 and 72 h, in different experimental setting. Experiments were subsequently done in 1% FBS. Unstimulated control cells (CTR) were grown in the same conditions of starvation i.e. 1% FBS. The effects of each treatment are referred to CTR. Two independent experiments were performed in triplicate.

Cell viability assessment

hPECs were cultured in 96-well collagen coated tissue culture plates and allowed to grow to 50% density in culture medium, switched to 1% FBS 24 h prior to experiment, to obtain synchronized quiescent cells. Viability was assessed at 24, 48 and 72 h of treatment with different concentration of BSA: 10 μg/ml, 100 μg/ml, 1 mg/ml, 10 mg/ml and 30 mg/ml by colorimetric assay (Methylene Blue assays)^{37–39}, as described above. Color stains only the cells attached to the substrate before fixation (i.e. living cells), thus allowing cell viability quantification.

In-Cell Western (ICW) assay

Protein expression was assessed in differentiated hPECs cultivated on collagen coated 96-well plates fixed with cold methanol for 10 min at RT after stimulation. Cells were washed five times for 10 min each with 0.1% Triton X-100 in 1X PBS, then blocked using 5% milk in 0.1% Triton X-100 in 1X PBS (blocking solution) for 40 min at RT with moderate shaking. Samples were incubated with primary antibody (Supplementary Table S1) diluted in

blocking solution at 4 °C overnight in a humidified chamber. After five washes with 0.1% Triton-X-100 in 1X PBS, secondary antibodies were diluted in blocking solution (Supplementary Table S1) and incubated for 1 h at RT with gentle shaking. The intensity of the labelled proteins was measured using the Odyssey CLx imaging system (LI-COR Biosciences—Lincoln, Nebraska USA). Negative controls were run by omitting primary antibody. Background values were obtained by omitting primary and secondary antibodies. Each experimental condition was run six independently times. Signals were normalized for the number of cells measured by Methylene Blue staining^{37–39}, as described above.

Morphological cell analysis

hPECs shape descriptors

For analysis of hPEC morphology, cells were seeded on eight-well chamber slides, cultured for 24, 48 and 72 h in normal condition (CTR) and BSA experimental treatments (10 and 30 mg/ml). After stimulation, hPECs were washed with 1X PBS and fixed with cold methanol for 10 min at RT. Changes in cell morphology were examined first under an inverted light phase contrast microscope (EVOS XL Core Cell Imaging System, Waltham, MA USA), that enabled a rapid analysis of cell culture status. Then, to obtain more morphological details, bright field microscopy of cells was performed with Leica DMI6000CS-TCS SP8 fluorescence microscope) with DIC 40X/0.60, and analyzed with LAS AF software. DIC optics creates a virtual relief image that appears as a pseudo 3D-effect, allowing the morphological analysis of transparent objects. Images were acquired using a DFC365FX camera (Leica Microsystems)³⁹. Pictures were taken at equal exposure times for each sample. Using DIC produces high resolution images with good contrast.

F-actin cytoskeleton staining and quantification

Actin cytoskeleton, was analyzed using phalloidin fluorescent staining. These evaluations were performed in basal conditions (not subjected to BSA treatment, CTR) and following albumin treatment (10 and 30 mg/ml) at 72 h. hPECs were chemically fixed using a 4% para-formaldehyde solution in 1X PBS. F-actin was stained using Phalloidin-iFluor-647 (ab176759, Abcam, Cambridge, UK) diluted 1:1000 in PBS for 1 h at RT. Nuclear counterstain was performed using DAPI diluted 1:1000 in PBS. Images were acquired using a Leica DMI6000CS-TCS SP8 fluorescence microscope with 20X/0.4 objective using a DFC365FX camera and LAS-AF software v.3.1.1 (Leica Microsystems).

The intensity of phalloidin signal was quantified in the different images using an area region of interest (ROI) and analyzed by LAS-AF software statistic calculation of the arithmetical mean of the measured gray-scale values. Each pixel in an image has a certain gray-scale value. Background raw integrated densities were subtracted, and this net integrated density was then normalized to the total cells number counted on the same measured cell area for untreated and treated hPECs.

Statistical analysis

Statistical analysis was performed using non-parametric tests (Mann–Whitney's U-test). Statistical significance was assessed using R software v.4.1.0⁴⁰. When indicated, comparisons among groups were obtained using one-way ANOVA with a between-within design and by Bonferroni's correction. Statistical significance was defined as a p value less than 0.05.

Data availability

Data is provided within the manuscript and in supplementary files.

Received: 18 March 2024; Accepted: 30 December 2024

Published online: 12 January 2025

References

- Zhao, X. et al. Albumin induces CD44 expression in glomerular parietal epithelial cells by activating extracellular signal-regulated kinase 1/2 pathway. *J. Cell Physiol.* **234**, 7224–7235 (2019).
- Bronstein, R., Pace, J., Gowthaman, Y., Salant, D. J. & Mallipattu, S. K. Podocyte-parietal epithelial cell interdependence in glomerular development and disease. *J. Am. Soc. Nephrol.* **34**, 737–750 (2023).
- Ceol, M. et al. Human parietal epithelial cells (PECs) and proteinuria in lupus nephritis: A role for ClC-5, megalin, and cubilin?. *J. Nephrol.* **36**, 2499–2506 (2023).
- Kietzmann, L. et al. MicroRNA-193a regulates the transdifferentiation of human parietal epithelial cells toward a podocyte phenotype. *J. Am. Soc. Nephrol.* **26**, 1389–1401 (2015).
- Kuppe, C. et al. Common histological patterns in glomerular epithelial cells in secondary focal segmental glomerulosclerosis. *Kidney Int.* **88**, 990–998 (2015).
- Ohse, T. et al. The enigmatic parietal epithelial cell is finally getting noticed: A review. *Kidney Int.* **76**, 1225–1238 (2009).
- Chang, A. M. et al. Albumin-induced apoptosis of glomerular parietal epithelial cells is modulated by extracellular signal-regulated kinase 1/2. *Nephrol. Dial. Transplant.* **27**, 1330–1343 (2012).
- D'Agati, V. D. & Shankland, S. J. Recognizing diversity in parietal epithelial cells. *Kidney Int.* **96**, 16–19 (2019).
- Wong, M. N., Tharaux, P.-L., Grahammer, F. & Puelles, V. G. Parietal epithelial cell dysfunction in crescentic glomerulonephritis. *Cell Tissue Res.* **385**, 345–354 (2021).
- Ceol, M. et al. Involvement of the tubular ClC-type exchanger ClC-5 in glomeruli of human proteinuric nephropathies. *PLoS ONE* **7**, e45605 (2012).
- Ronconi, E. et al. Regeneration of glomerular podocytes by human renal progenitors. *J. Am. Soc. Nephrol.* **20**, 322–332 (2009).
- Lasagni, L. & Romagnani, P. Basic research: Podocyte progenitors and ectopic podocytes. *Nat. Rev. Nephrol.* **9**, 715–716 (2013).
- Cui, S., Verroust, P. J., Moestrup, S. K. & Christensen, E. I. Megalin/gp330 mediates uptake of albumin in renal proximal tubule. *Am. J. Physiol.* **271**, F900–907 (1996).
- Zhai, X. Y. et al. Cubilin- and megalin-mediated uptake of albumin in cultured proximal tubule cells of opossum kidney. *Kidney Int.* **58**, 1523–1533 (2000).

15. Ganesello, L. et al. Albumin uptake in human podocytes: a possible role for the cubilin-amnionless (CUBAM) complex. *Sci. Rep.* **7**, 13705 (2017).
16. Chin, V. T. et al. Rho-associated kinase signalling and the cancer microenvironment: Novel biological implications and therapeutic opportunities. *Expert Rev. Mol. Med.* **17**, e17 (2015).
17. Porazinski, S., Parkin, A. & Pajic, M. Rho-ROCK signaling in normal physiology and as a key player in shaping the tumor microenvironment. *Adv. Exp. Med. Biol.* **1223**, 99–127 (2020).
18. Rbaibi, Y. et al. Megalin, cubilin, and Dab2 drive endocytic flux in kidney proximal tubule cells. *Mol. Biol. Cell* **34**, ar74 (2023).
19. Sagrinati, C. et al. Isolation and characterization of multipotent progenitor cells from the Bowman's capsule of adult human kidneys. *J. Am. Soc. Nephrol.* **17**, 2443–2456 (2006).
20. Eymael, J. et al. CD44 is required for the pathogenesis of experimental crescentic glomerulonephritis and collapsing focal segmental glomerulosclerosis. *Kidney Int.* **93**, 626–642 (2018).
21. Froes, B. P. et al. Is CD44 in glomerular parietal epithelial cells a pathological marker of renal function deterioration in primary focal segmental glomerulosclerosis?. *Pediatr. Nephrol.* **32**, 2165–2169 (2017).
22. Okamura, K. et al. Endocytosis of albumin by podocytes elicits an inflammatory response and induces apoptotic cell death. *PLoS ONE* **8**, e54817 (2013).
23. Ohse, T. et al. Albumin induces endoplasmic reticulum stress and apoptosis in renal proximal tubular cells. *Kidney Int.* **70**, 1447–1455 (2006).
24. Erkan, E., De Leon, M. & Devarajan, P. Albumin overload induces apoptosis in LLC-PK1 cells. *Am. J. Physiol.-Renal Physiol.* **280**, F1107–F1114 (2001).
25. Amin, E. et al. Rho-kinase: Regulation, (dys)function, and inhibition. *Biol. Chem.* **394**, 1399–1410 (2013).
26. Asp, P., Wihlborg, M., Karlén, M. & Farrants, A.-K.O. Expression of BRG1, a human SWI/SNF component, affects the organisation of actin filaments through the RhoA signalling pathway. *J. Cell Sci.* **115**, 2735–2746 (2002).
27. Rath, N. & Olson, M. F. Rho-associated kinases in tumorigenesis: Re-considering ROCK inhibition for cancer therapy. *EMBO Rep.* **13**, 900–908 (2012).
28. Kadir, S., Astin, J. W., Tahtamouni, L., Martin, P. & Nobes, C. D. Microtubule remodelling is required for the front-rear polarity switch during contact inhibition of locomotion. *J. Cell Sci.* **124**, 2642–2653 (2011).
29. Coleman, M. L. et al. Membrane blebbing during apoptosis results from caspase-mediated activation of ROCK I. *Nat. Cell Biol.* **3**, 339–345 (2001).
30. Sebbagh, M. et al. Caspase-3-mediated cleavage of ROCK I induces MLC phosphorylation and apoptotic membrane blebbing. *Nat. Cell Biol.* **3**, 346–352 (2001).
31. Shi, J. & Wei, L. Rho kinase in the regulation of cell death and survival. *Arch. Immunol. Ther. Exp. (Warsz)* **55**, 61–75 (2007).
32. Orlando, K. A., Stone, N. L. & Pittman, R. N. Rho kinase regulates fragmentation and phagocytosis of apoptotic cells. *Exp. Cell Res.* **312**, 5–15 (2006).
33. Street, C. A. & Bryan, B. A. Rho kinase proteins—Pleiotropic modulators of cell survival and apoptosis. *Anticancer Res.* **31**, 3645–3657 (2011).
34. Shimizu, A. et al. Apoptosis in the repair process of experimental proliferative glomerulonephritis. *Kidney Int.* **47**, 114–121 (1995).
35. Sicking, E.-M. et al. Subtotal ablation of parietal epithelial cells induces crescent formation. *J. Am. Soc. Nephrol.* **23**, 629–640 (2012).
36. Coffey, S., Costacou, T., Orchard, T. & Erkan, E. Akt links insulin signaling to albumin endocytosis in proximal tubule epithelial cells. *PLoS ONE* **10**, e0140417 (2015).
37. Oliver, M. H., Harrison, N. K., Bishop, J. E., Cole, P. J. & Laurent, G. J. A rapid and convenient assay for counting cells cultured in microwell plates: application for assessment of growth factors. *J. Cell Sci.* **92**, 513–518 (1989).
38. Priante, G. et al. Caspase-independent programmed cell death triggers Ca₂PO₄ deposition in an in vitro model of nephrocalcinosis. *Biosci. Rep.* **38**, BSR20171228 (2018).
39. Priante, G. et al. Human proximal tubular cells can form calcium phosphate deposits in osteogenic culture: Role of cell death and osteoblast-like transdifferentiation. *Cell Death Discov.* **5**, 57 (2019).
40. R Core Team.—European Environment Agency (2020). <https://www.eea.europa.eu/data-and-maps/indicators/oxygen-consumin-g-substances-in-rivers/r-development-core-team-2006>.

Acknowledgements

To Catherine Meyer-Schwesinger that give us the human Parietal Epithelial Cells.

Author contributions

D.D.P., L.G., and F.A. study conception; G.P., L.G. and M.C.^a design experiments; G.P., L.G., M.C.^a and R.M. conducted the experiments; C.M.R. provided assistance with the experimental methodology; L.G., and G.P. conducted statistical analysis; G.P. prepared the table and illustrative figures; F.N., L.F.S., M.C.^b, F.K.M., G.P. and M.C.^a contributed to the literature review; G.P., F.A., M.C.^a, L.G., L.A.C., and D.D.P. critically reviewed the results; G.P., F.A., M.C.^a, L.G., and D.D.P. wrote the manuscript. All authors have read and agreed to the published version of the manuscript. (M.C.^a Monica Ceol; M.C.^b Martina Cacciapuoti)

Funding

This research was supported by the University of Padua, and DOR2322480 awarded to D.D.P.

Declarations

Competing interests

The authors declare no competing interests.

Additional information

Supplementary Information The online version contains supplementary material available at <https://doi.org/10.1038/s41598-024-84972-2>.

Correspondence and requests for materials should be addressed to G.P.

Reprints and permissions information is available at www.nature.com/reprints.

Publisher's note Springer Nature remains neutral with regard to jurisdictional claims in published maps and institutional affiliations.

Open Access This article is licensed under a Creative Commons Attribution-NonCommercial-NoDerivatives 4.0 International License, which permits any non-commercial use, sharing, distribution and reproduction in any medium or format, as long as you give appropriate credit to the original author(s) and the source, provide a link to the Creative Commons licence, and indicate if you modified the licensed material. You do not have permission under this licence to share adapted material derived from this article or parts of it. The images or other third party material in this article are included in the article's Creative Commons licence, unless indicated otherwise in a credit line to the material. If material is not included in the article's Creative Commons licence and your intended use is not permitted by statutory regulation or exceeds the permitted use, you will need to obtain permission directly from the copyright holder. To view a copy of this licence, visit <http://creativecommons.org/licenses/by-nc-nd/4.0/>.

© The Author(s) 2025